

Cite this: *Nanoscale*, 2014, **6**, 15098

A new phase transformation path from nanodiamond to new-diamond via an intermediate carbon onion[†]

J. Xiao,[‡] J. L. Li,[‡] P. Liu and G. W. Yang*

The investigation of carbon allotropes such as graphite, diamond, fullerenes, nanotubes and carbon onions and mechanisms that underlie their mutual phase transformation is a long-standing problem of great fundamental importance. New diamond (n-diamond) is a novel metastable phase of carbon with a face-centered cubic structure; it is called "new diamond" because many reflections in its electron diffraction pattern are similar to those of diamond. However, producing n-diamond from raw carbon materials has so far been challenging due to n-diamond's higher formation energy than that of diamond. Here, we, for the first time, demonstrate a new phase transformation path from nanodiamond to n-diamond via an intermediate carbon onion in the unique process of laser ablation in water, and establish that water plays a crucial role in the formation of n-diamond. When a laser irradiates colloidal suspensions of nanodiamonds at ambient pressure and room temperature, nanodiamonds are first transformed into carbon onions serving as an intermediate phase, and sequentially carbon onions are transformed into n-diamonds driven by the laser-induced high temperature and high pressure from the carbon onion as a nanoscaled temperature and pressure cell upon the process of laser irradiation in a liquid. This phase transformation not only provides new insight into the physical mechanism involved, but also offers one suitable opportunity for breaking controllable pathways between n-diamond and carbon allotropes such as diamond and carbon onions.

Received 10th September 2014,
Accepted 12th October 2014

DOI: 10.1039/c4nr05246c
www.rsc.org/nanoscale

1. Introduction

The phase transformation between diamond and other carbon allotropes, for example graphite, fullerenes, nanotubes and carbon onions, has been of intense interest from the viewpoints of science and technology for a century, and breaking controllable pathways between diamond and these carbon allotropes is a subject that has fascinated scientists and engineers for several decades.^{1–10} Among the multifarious carbon allotropes, a novel metastable phase of carbon with a face-centered cubic (fcc) structure has been produced by some techniques under extreme conditions.^{11–13} This unique form of carbon is called new diamond (n-diamond) because many reflections in its electron diffraction pattern are similar to those of diamond.¹¹ In recent years, this metastable phase of

carbon has attracted considerable interest because researchers have demonstrated that n-diamond actually presents a new kind of metastable phase of carbon with the fcc structure and is expected to have great potential applications in areas of mechanical engineering, microelectronics and optoelectronics.^{11–15} Therefore, there is growing interest in breaking controllable pathways between n-diamond and other carbon allotropes including graphite and diamond. However, producing n-diamond from raw carbon materials has so far been challenging due to n-diamond's higher formation energy than that of diamond.¹⁶

Here, we, for the first time, demonstrate a new phase transformation pathway from nanodiamond to n-diamond *via* an intermediate carbon onion driven by the process of laser ablation in water, and we establish that water plays a crucial role in the formation of n-diamond. These results reveal a series of phase transformations between n-diamond and other carbon allotropes such as diamond and carbon onions, and provide a clear and general insight into the basic physics involved in these conversions. Meanwhile, this phase transformation path from diamond to n-diamond opens up avenues for producing n-diamond from raw carbon materials.

State Key Laboratory of Optoelectronic Materials and Technologies, Institute of Optoelectronic and Functional Composite Materials, Nanotechnology Research Center, School of Physics & Engineering, Sun Yat-Sen University, Guangzhou 510275, Guangdong, P. R. China. E-mail: stsygw@mail.sysu.edu.cn

[†] Electronic supplementary information (ESI) available. See DOI: 10.1039/c4nr05246c
[‡] These authors contributed equally to this work.

2. Experimental

In our study, raw detonation nanodiamonds (Aldrich, $\geq 97\%$ trace metal basis, nanopowder) synthesized from the detonation of a mixture of trinitrotoluene and hexogen⁹ and deionized water are used without further purification. The experiments are carried out in a system of laser ablation in a liquid.^{17,18} In this case, about 3 mg raw detonation nanodiamonds are dropped into a 10 mL bottle filled with deionized water to form a suspension. Then, a second harmonic of 1 mm beam size produced using a Q-switched Nd:YAG laser device with a wavelength of 532 nm, a pulse width of 10 ns, a repeating frequency of 10 Hz, and a laser pulse power of 200 mJ is focused into the middle of the bottle. During the laser irradiation, the solution was stirred with a magnetic stirrer. After the ablation, one drop of the solution synthesized by different period is pipetted onto a carbon support film on a copper grid for transmission electron microscopy (TEM) observation. TEM and high resolution transmission electron microscopy (HRTEM) images are recorded using an FEI Tecnai G2 F30 transmission electron microscope equipped with a field-emission gun. The electron energy loss spectra (EELS) are recorded using an imaging filter (Gatan GIF) in the TEM imaging mode. The energy resolution of the system is 1 eV (FWHM of a zero-loss peak) and the maximum dispersion is 0.05 eV per channel.

All the theoretical calculations are performed using the DMOL package. Spin unrestricted calculations in the generalized gradient approximation (GGA) with the Perdew–Burke–Ernzerhof (PBE) exchange-correlation function are performed. The atomic orbital basis set is of double-numerical quality with inclusion of polarization functions (DNP). The configurations are fully relaxed without any symmetric constraints until the maximal forces are less than 0.002 hartree Å⁻¹. The Kohn–Sham equations are solved self-consistently with a convergence of 10⁻⁵ Ha on the total energy. The potential energy profile of the face-centered cubic carbon is scanned using different lattice constants. The completely same theoretical-level calculations are performed for diamond.

The EELS of the face-centered cubic carbon is calculated using the CASTEP package. The calculations adopted the GGA with the PBE exchange-correlation function. The Kohn–Sham equations are solved self-consistently with a convergence of 10⁻⁵ Ha (1 Ha = 27.2116 eV) on the total energy. The kinetic energy cut-off is 350 eV. A core hole calculation is performed in a 3 × 3 × 3 supercell to ensure that one single cell only contains one full core hole. The pseudopotential constructed for an atom missing a core electron is on the fly (OTFG) and in the representation of reciprocal space. To ensure this issue, we carried out the same theoretical-level calculation for the EELS of diamond.

3. Results and discussion

Fig. 1a shows the typical morphology of aggregated raw nanodiamonds with a size of about 5 nm. Four strong diffraction

rings (Fig. 1b) represent the (111), (220), (311), (400) planes of diamond. The HRTEM image of raw nanodiamonds consists of the crystalline diamond cores and the amorphous outer shells as shown in Fig. 1c. Scanning transmission electron microscopy (STEM) (Fig. 1(d, e)) and TEM images (Fig. 1(g, h)) demonstrate that the as-synthesized products turned out to be nanoparticles with diameters of 30–40 nm and these nanoparticles are in the shape of nanospheres connected to each other. In spite of the similarity of the crystal lattice parameter of the phase to that of diamond, its selected area electron diffraction (SAED) pattern significantly differs from that of diamond as shown in Fig. 1f. Four strong diffraction rings represent the (111), (200), (220) and (311) planes of n-diamonds. Note that the (200) ring of n-diamond is forbidden for diamond.¹⁹ In the HRTEM image of n-diamonds (Fig. 1i), we can see that these n-diamonds are embedded into the disordered carbons. This phenomenon is concerned with the stability of sp³ bonding, which is discussed in detail below. The ratio between amorphous carbon and n-diamond is roughly estimated to be 7 : 3. Besides, some nanodiamonds are consumed in other ways, such as vaporization and transformation to organic groups, when subjected to laser ablation. Therefore, combining these influencing factors, the percent conversion between raw diamond and n-diamond is approximately 10%. Furthermore, HRTEM analysis of the individual n-diamond (Fig. 1j, k) shows that the two interplanar spacings of 0.313 and 0.272 nm, respectively, correspond to the crystallographic planes of the (111) and (200) of the fcc structure quite well. In addition, an angle of $\Phi = 125^\circ$ between the two interplanar spacings further confirms that the as-synthesized samples possess a fcc structure with a lattice parameter of 0.545 nm. Accordingly, TEM data demonstrate a phase transformation from diamond to n-diamond. Note that the n-diamond synthesized by this method is different from the common n-diamond reported in the literature.^{11–15} The difference between these three diamond structures is listed in Table 1. Additionally, we compare and estimate their stability by introducing first-principles calculation, and these results show that the total formation energy of the n-diamond in our case is higher, 0.65 and 1.05 Ha (1 Ha = 27.2116 eV), than that of the common n-diamond and diamond, respectively, which means that the n-diamond with a larger lattice parameter ($a = 0.545$ nm) in our case is a metastable state compared to other two diamonds ($a = 0.356$ nm) (the detailed calculation is in ESI†).

In order to elucidate in detail the phase transformation process above, we carefully checked the products under different irradiation of the laser stage and found the intermediate products formed during the diamond to n-diamond transition. The irradiation time for nine bottles shown in Fig. 2e is 0, 5, 10, 15, 20, 45, 60, 70 and 90 min, respectively. The sample of the final products is taken from the 9th bottle in Fig. 2e. HRTEM images of the intermediate products in Fig. 2 show various morphologies of carbon onions (the sample from the 5th bottle in Fig. 2e) including quasi-spherical particles, polyhedron particles with closed concentric graphite shells,

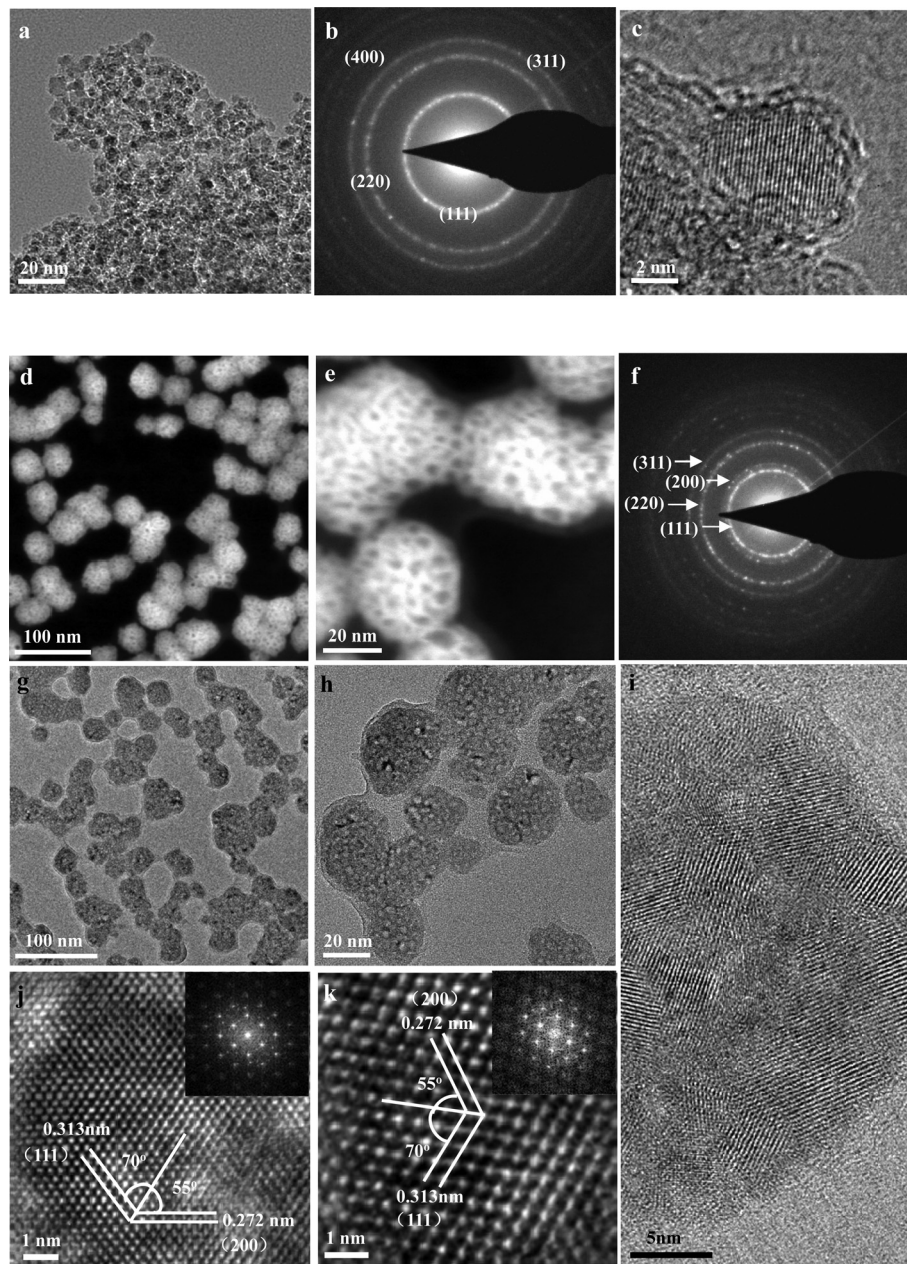


Fig. 1 Microscopy characterization of nanodiamonds and n-nanodiamonds. (a) Typical morphology of aggregated raw nanodiamonds with a size of about 5 nm. (b) Four strong diffraction rings representing the (111), (220), (311), (400) planes of diamond. (c) HRTEM image of raw nanodiamonds covered with the amorphous carbon shell. (d, e) Low and high magnification STEM images of n-nanodiamonds. (f) SAED pattern of n-nanodiamonds. Four strong diffraction rings denoting the (111), (200), (220), (311) planes of n-nanodiamonds. Note that the (200) ring is forbidden for diamond. (g, h) Low and high resolution TEM images of n-nanodiamonds. (i) HRTEM image of n-nanodiamonds. These n-nanodiamonds are found to be embedded in the disordered carbons. (j, k) HRTEM image of the individual n-nanodiamond. Detailed analysis showing the marked lattice spacing measured to be 0.313 and 0.272 nm, respectively, which coincides with the d value of the (111) and (200) lattice planes of diamond with a face-centred cubic structure. The interfacial angle of $\sim 125^\circ$ also confirms this structure.

and elongated particles with linked external graphite-like layers. Clearly, the spacing of the lattice fringes is about 0.34 nm, corresponding to that of the (002) plane of graphite. These results thus show that raw nanodiamonds are first transformed into carbon onions serving as an intermediate phase, and sequentially carbon onions are transformed into n-diamonds in the process of laser irradiation in a liquid. During the laser

irradiation, we can clearly see a series of significant color changes in the colloid from opaque grayish white to dark black and finally to a transparent colorless colloid as shown in Fig. 2e. Note that the intermediate phase is black in both water and alcohol environments,¹⁷ which indicates that carbon onions can be definitely regarded as the transient phase from raw nanodiamonds to the final products no matter in what kind of liquid.

Table 1 Indexing results of SAED patterns of various diamond nanostructures^a

(hkl)	$D_{\text{exp.}} (\text{\AA})$	$D_{\text{theor.}} (\text{\AA})$
(a) Diamond $a = 3.56 \text{\AA}$		
111	2.06	2.05
220	1.27	1.26
311	1.09	1.07
400	0.90	0.89
(b) Common n-diamond ³⁰ $a = 3.56 \text{\AA}$		
111	2.09	2.06
200	1.79	1.78
220	1.27	1.26
311	1.10	1.07
(c) n-Diamond in our case $a = 5.45 \text{\AA}$		
111	3.13	3.15
200	2.72	2.73
220	1.92	1.93
311	1.64	1.64

^a $D_{\text{exp.}}$ refers to the experimental values. $D_{\text{theor.}}$ refers to the theoretical values. a refers to the lattice parameter.

Fig. 3a shows the EELS spectra of nanodiamond, carbon onions and n-diamond, respectively. The curve (i) in Fig. 3a gives a characteristic diamond peak >290 eV, due to the transition from the 1s core level to the σ^* band ($1s \rightarrow \sigma^*$ transition),²⁰ apart from the presence of a weak peak at 284.8 eV ($1s \rightarrow \pi^*$ transition). These results indicate the presence of some sp^2 -bonded carbon atoms, which is verified by TEM observation in Fig. 1c. Despite the ordered network of carbon onions observed in HRTEM images (Fig. 2(a-d)), this EELS characterized by the carbon K edge (the curve (ii) in Fig. 3) resembles that obtained for amorphous carbon.²¹ The broadened peak at 284.8 eV corresponds to the transition from the 1s core level to the π^* band ($1s \rightarrow \pi^*$ transition), and no obvious peaks appear above 290 eV, suggesting that sp^3 bonds transform into sp^2 bonds. This phenomenon corresponds well to that of Tomita's research.²² In the spectrum of n-diamonds (the curve (iii) in Fig. 3), we can see a shoulder at about 284.8 eV. The disordered carbons as shown in Fig. 1i are considered to be responsible for the shoulder. However, the fine structure above the $1s \rightarrow \sigma^*$ transition observed for n-diamonds is significantly different from that of common nanodiamonds in the relative intensity and peak location. The three characteristic $1s \rightarrow \sigma^*$ transitions at 291.9, 297.7, and 305.3 eV shifted to 291.7, 302.8, and 314.2 eV, respectively. In order to validate the accuracy of experimental observations, we performed the DFT calculations to simulate the EELS spectra (the detailed process is in ESI†). Firstly, we obtained the EELS spectrum of well-known diamond as shown in Fig. 3b. Clearly, the theoretical results are consistent with those of the experimental measurement. Therefore, this simulation method is recognized to be convincing and reliable. Then, the EELS spectrum of n-diamond is calculated based on the same method as shown in Fig. 3c. The shape and relative intensity of three peaks are basically the same as that of the experimental profile. Although the theoretical values of peak locations are in

disparity with the experimental values due to the calculation issues, it would not influence the precision in judging the shape and relative intensity of peaks, which have been validated by testing the EELS spectrum of diamond (Fig. 3b). Therefore, combining experimental and theoretical data, we confirm that the products are n-diamonds with a face-centred cubic structure.

To further confirm the phase transformation processes, we utilize the UV Raman spectroscopy (325 nm) to analyse samples collected at different stages, as shown in Fig. 4. Raw detonation nanodiamonds (bottom) show a peak at 1325 cm^{-1} , which is a typical signal of diamond,⁹ and the G band peaks around 1600 cm^{-1} . After 20 min ablation, the diamond peak upshifts to about 1410 cm^{-1} , which is attributed to the disordered sp^2 -bonded carbon phase (D band).²³ Besides, due to the effect of the shell curvature of carbon onions, the G band downshifts to 1585 cm^{-1} (middle). Finally, the D band moves down to 1363 cm^{-1} (top). Although the amorphous carbon around n-diamond has some influence on the final Raman signal of n-diamond, the downshift of the D band is still considered to be due to the increase of sp^3 bonding when generating n-diamonds.¹⁷

Based on the above detailed characterization, the as-synthesized products are confirmed to be the n-diamond formed by laser ablating raw detonation nanodiamonds in deionized water. However, according to our previous research,¹⁷ when the liquid used is absolute alcohol, the final products are common nanodiamonds with good monodispersity. Therefore, it is obvious that the liquid is a key factor in determining the final carbon structure. Gogotsi *et al.* have claimed that the surface of sp^3 clusters must be either stabilized through termination with functional groups or reconstructed into sp^2 carbon.⁹ In order to judge the surface termination of the products synthesized with different liquids, Fourier transform infrared spectroscopy (FTIR) was introduced as shown in Fig. 5. The functional groups present in diamonds synthesized in alcohol are C=O, COOR, C–O–C, OH and C–H groups, which are much more than OH and few C–H and C–O groups of n-diamond synthesized in water. Back to Gogotsi's claim, in order to retain the stability of surface sp^3 clusters, the diamonds synthesized in the alcohol environment remained stable by means of various kinds of groups adsorbed on their surfaces. In particular for carboxyl and carbonyl groups (not found in the water environment), they seem to easily adhere to the surface of the carbon backbone.^{25,26} Due to the lack of functionalities in the relatively moderate water environment, the bare (non-functionalized) or less-functionalized surfaces of the diamonds exhibit structures similar to bulk diamond. The surfaces of octahedral, cuboctahedral and spherical clusters show a transition from sp^3 carbon to sp^2 carbon,²⁷ which corresponds to our EELS analysis and TEM observation. Thus, these results prove the existence of the disordered carbons around n-diamond, which play an important role in the stability of n-diamonds by influencing surface reconstruction by taking the shape of sp^2 carbons.

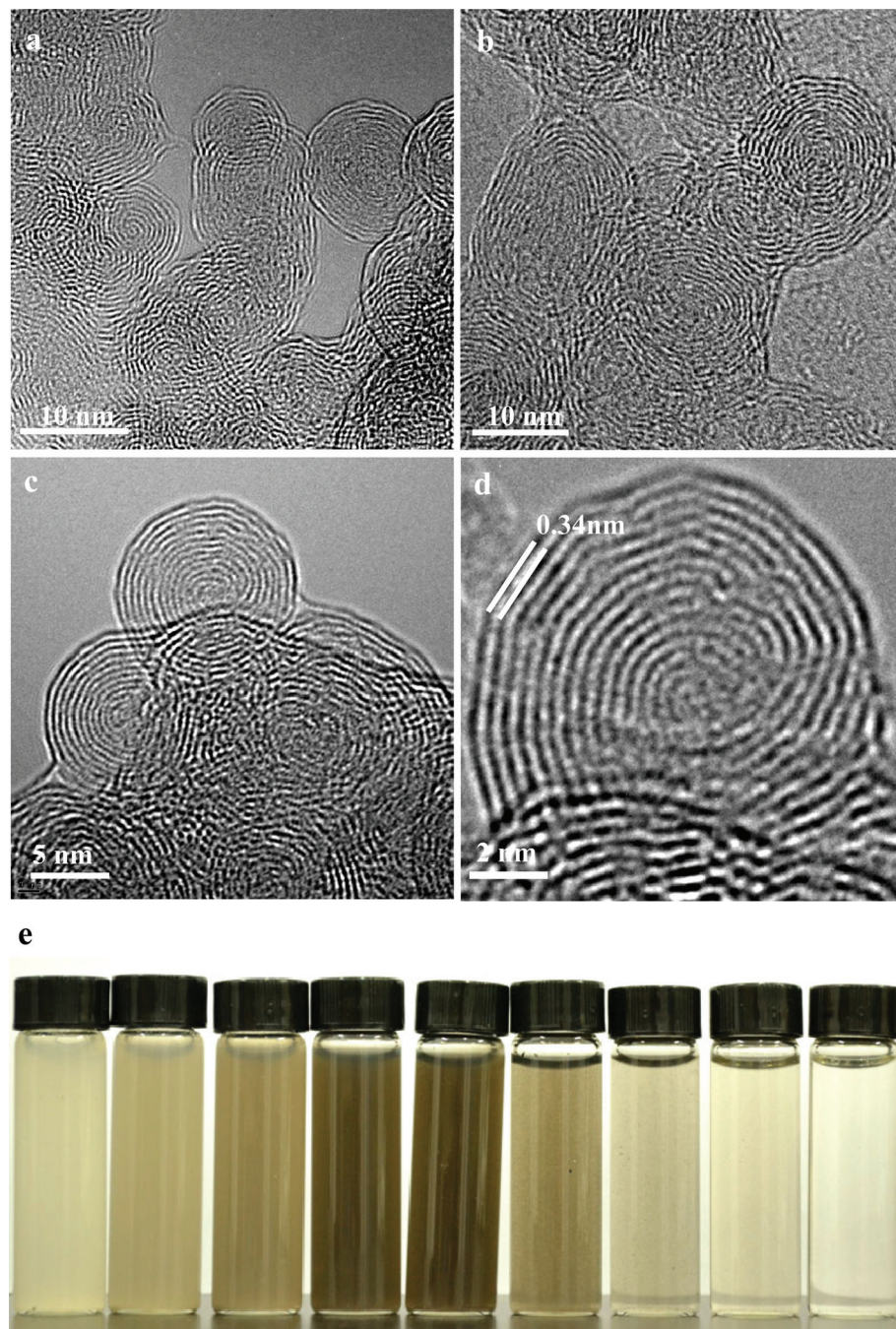


Fig. 2 Carbon onion serving as the intermediate phase. (a–d) The spherical carbon onions aggregated, which contain quasi-spherical particles with closed concentric graphite shells, elongated particles with linked external graphite-like layers and closed quasi-spherical internal shells. The interplanar spacing of 0.34 nm corresponds to that of the (002) plane of graphite. (e) Color change with the increase of laser irradiation time. Clearly, the color of the solution changes from opaque greyish white to dark black and finally to a transparent colorless solution.

In addition, another aspect worth pointing out is that the as-synthesized n-diamond has higher formation energy than diamond. We have successfully synthesized the cubic structure carbon from laser ablation amorphous carbon films in water such as C₈ nanocubes and body-centered cubic carbon nanocrystals.^{28,29} Recently, C₈ carbon and common n-diamonds are generated using an ArF excimer laser in deionized water.³⁰ These studies all confirm that the water environment plays an impor-

tant role in forming metastable carbon structures. Although the effect of water on diamond phase is unclear so far, hydroxyl derived from water may prompt diamond up to a metastable phase with higher level. Considering FTIR results, we find that the hydroxyls adsorbed on n-diamond are more than those in the alcohol environment, which corresponds to our deductions.

As is well known, the carbon onion is the stable form of carbon at ambient temperature and pressure, and both the

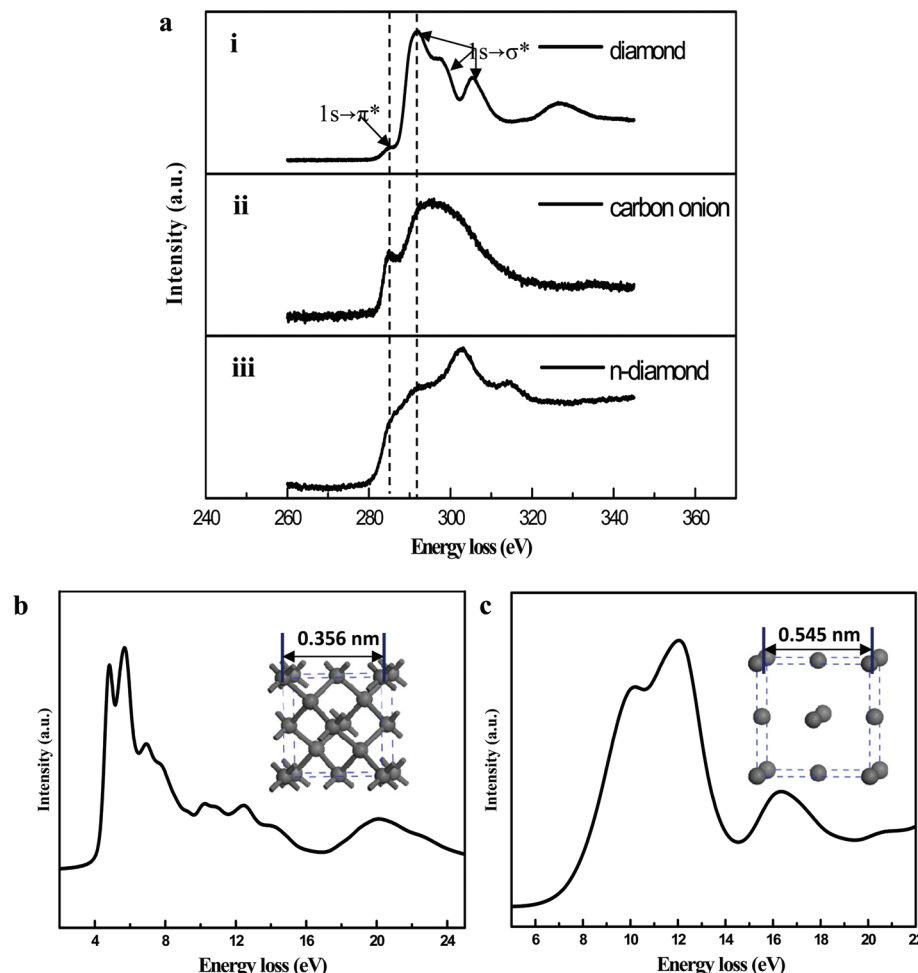


Fig. 3 EELS analysis. (a) Experimental comparison of nanodiamond, carbon onions and n-nanodiamond. All these spectra show the same peak at about 284.8 eV, meaning that these samples are involved in the $1s \rightarrow \pi^*$ transition. However, they are significantly different in the $1s \rightarrow \sigma^*$ transition. (b, c) The theoretical modeling of diamond and n-diamond, respectively; the inset shows the corresponding crystal structure.

diamond and n-diamond are metastable.³¹ Thus, diamonds can be converted to carbon onions by a simple thermal annealing.³² However, according to our calculations, the formation energy of n-diamond is even higher than that of diamond, which means that n-diamond is metastable compared with diamond. Therefore, the thermodynamic driving force (high temperature and high pressure) is needed to push carbon onions to convert into n-diamond.

During the laser irradiation of the starting nanodiamonds with thin amorphous carbon shells, the laser can induce a high temperature in the amorphous carbon shell by amorphous carbon absorption of laser energy.³³ Therefore, we first establish a heating model of nanoparticles upon laser irradiation in a liquid on the basis that amorphous carbon and carbon onions can absorb light and be heated.³³ The energy absorbed by a nanoparticle from the laser pulse is spent in the heating process, which is described in the following equation¹⁷

$$J\sigma_{\text{abs}}^{\lambda} = m \int_{T_0}^T C_p(T) dT \quad (1)$$

where m is the particle mass, d is the diameter of particles, ρ is the density, J is the laser fluence, T_0 is the temperature fixed at 300 K, $\sigma_{\text{abs}}^{\lambda}$ is the particle absorption cross-section which strongly depends on the laser wavelength, and $C_p(T)$ is the heat capacity. From eqn (1), it is clear that the amorphous carbon shell can be heated by supplying sufficient power with a laser. This situation applies equally to carbon onions. For detailed theoretical modeling of laser-induced high temperature in amorphous carbon and carbon onions one can refer to ESI S1 and Fig. S1–S4.†

Similarly, a laser can induce a high temperature in these carbon onions by carbon onion absorption of laser energy on the basis of the proposed theoretical model. However, this laser-induced high temperature will compress the interlayer distance of carbon onions. Finally, the interlayer distance reduction will result in a high pressure inside carbon onions.¹⁷ Therefore, carbon onions can be regarded as a nanoscaled temperature and pressure cell upon the process of laser irradiation in a liquid. A theoretical model was developed to pursue the origin of high pressure inside carbon onions in our case.

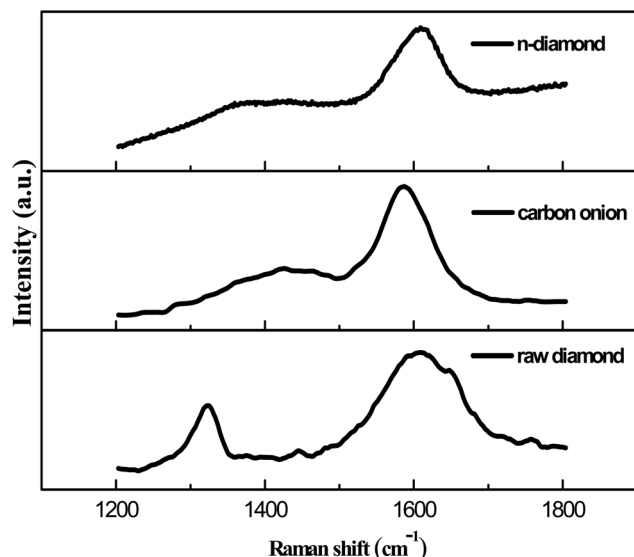


Fig. 4 Raman spectral analysis of the phase transformation from the raw nanodiamonds to the n-diamond. Raw detonation nanodiamonds (bottom), a peak at 1325 cm^{-1} is a typical signal of diamond and the G band peaks around 1600 cm^{-1} . After the appearance of carbon onions (middle), the diamond peak shifts to 1410 cm^{-1} , the G band also makes a downshift to 1585 cm^{-1} . The peak at $\sim 1410\text{ cm}^{-1}$ downshifting to 1363 cm^{-1} is associated with generation of n-diamond (top), probably ascribed to the increase of sp^3 bonding.

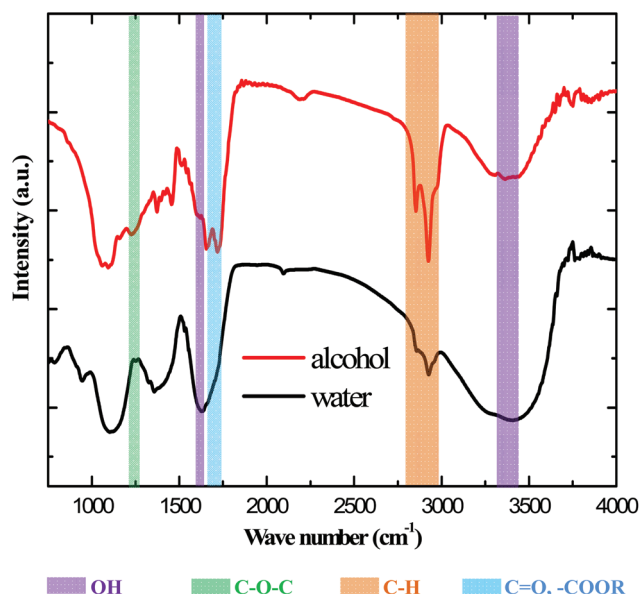


Fig. 5 FTIR spectrum of products synthesized in alcohol and water, respectively, showing the samples synthesized in the alcohol environment having much more functional groups than water.

Considering a carbon onion consisting of a cage with radius R , the pressure (p) acting on carbon cages is^{17,34}

$$p = \frac{\rho_\infty^2}{4\pi R^2} \int_{S^{(0)}} \left(\int_{S_i^{(0)}} F dS^{(0)} \right) dS^{(0)} \quad (2)$$

where ρ_∞ is the atom density of plane graphene, $S^{(0)}$ denotes the area of carbon cages in the undeformed state which is used as a reference configuration, and F is the vdW force acting on each of the atoms (positive for the attraction). For detailed theoretical modeling of a laser-induced high-pressure environment inside the carbon onion one can refer to ESI S2 and Fig. S5–S7.[†]

According to the recent review regarding transformation of carbon nanoparticles, the nucleation of diamond cores in carbon onions is observed when the onions are exposed to sustained electron irradiation above $400\text{ }^\circ\text{C}$ and the pressure in the centre of the onion is estimated to be clearly above 10 GPa .³⁵ From Fig. S4 and S7,[†] a high temperature and high pressure induced by the laser will lead to more than $2000\text{ }^\circ\text{C}$ and 20 GPa inside carbon onions. Therefore, considering a high-temperature and high-pressure environment inside carbon onions driven by the laser irradiation in a liquid coupled with a unique water environment discussed above, it is very reasonable to realize the carbon nanoparticles with higher formation energy than diamond, such as n-diamond in our case.

In order to verify the possibility whether the onions can transform into n-diamonds, we synthesize pure carbon onions by annealing the nanodiamonds at $1500\text{ }^\circ\text{C}$ in a high vacuum chamber ($\sim 10^{-3}\text{ Pa}$) for 30 min, which is similar to previous work by other authors.^{21,32} After heating treatment, the brown powder became dark black (Fig. 6a). We took about 3 mg samples into the bottle filled with deionized water and carried out similar laser irradiation in a liquid. A series of significant color changes in the colloid from dark black to a transparent colorless colloid during the laser irradiation were observed (Fig. 6b). This phenomenon of color change is identical to the latter part shown in Fig. 2e. Sequentially, the products after annealing and the final products were taken for TEM characterization. The black products turned out to be carbon onions (Fig. 6c), which is in good agreement with the previous results.^{21,32} Besides, n-diamonds can still be found in the final bottles, which was confirmed from HRTEM images and SAED patterns (Fig. 6d). This verification test demonstrates that the onions can transform directly into n-diamond. In other words, this phase transformation mechanism from nanodiamonds to onions to n-diamond is confirmed to be evidencing and convincing.

Based on the experimental observation and the corresponding thermodynamic analysis above, the phase transformation path from diamond to n-diamond *via* an intermediate carbon onion in the process of laser irradiation in a liquid is described as shown in Fig. 7. In the nanodiamond to carbon onion phase transformation, the laser can induce a high temperature in the amorphous carbon shell by amorphous carbon absorption of laser energy during the laser irradiation of the starting nanodiamonds with thin amorphous carbon shells in a liquid. Then, the laser-induced high temperature induces the nanodiamond core to transform into the carbon onion. Sequentially, the laser irradiates the carbon onion and then drives it into a state of high temperature by carbon onion

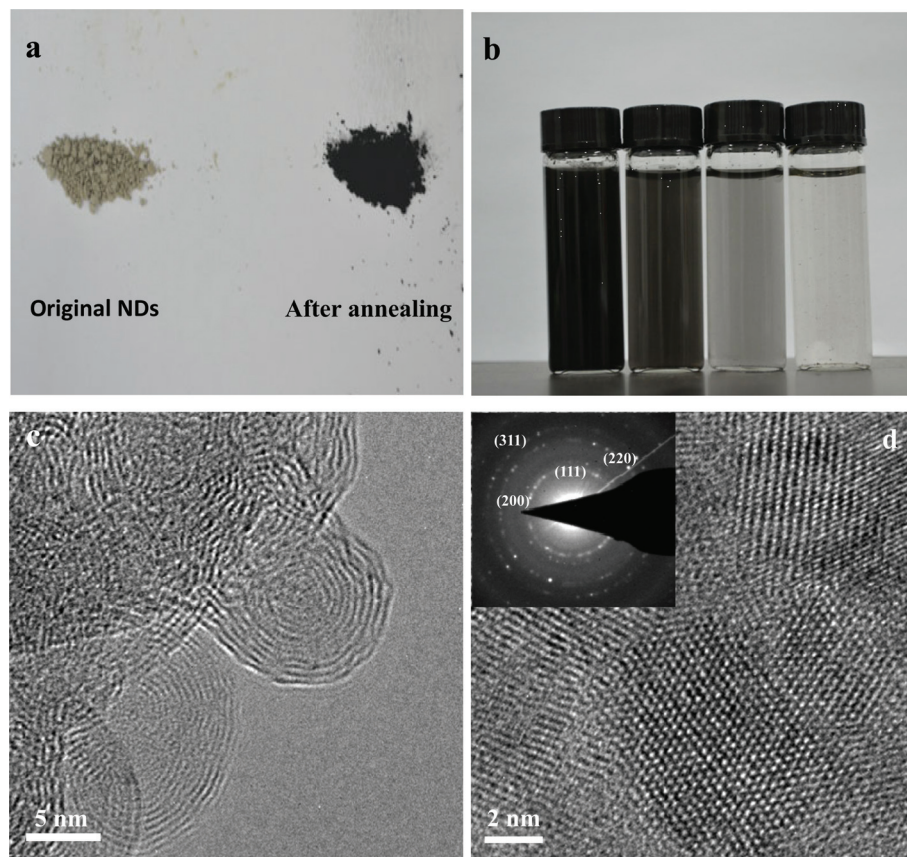


Fig. 6 Direct transformation from carbon onions to n-diamonds. (a) Annealing of the brown nanodiamonds (left) at 1500 °C in a high vacuum chamber, the color of products became dark black (right). (b) A series of significant color changes of the colloid from dark black to a transparent colorless colloid during the laser irradiation. (c) The HRTEM image of products after heating treatment, which turns out to be carbon onions. (d) The SAED pattern and HRTEM image of the final products, matching with the structure of n-diamond.

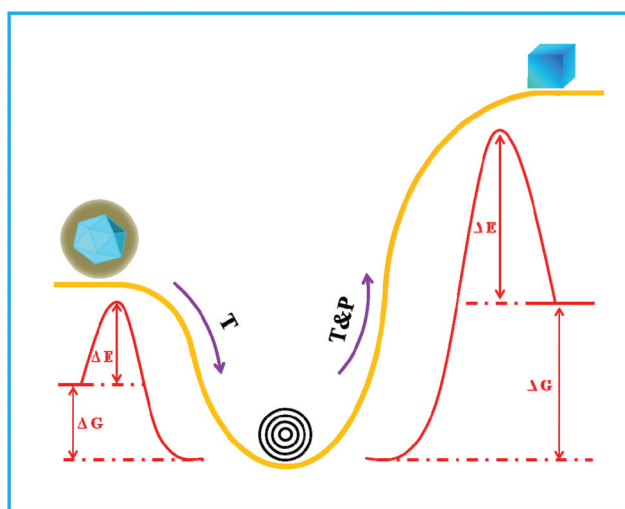


Fig. 7 Schematic illustration of the physical mechanism of the phase transformation from nanodiamond to n-nanodiamond. ΔG means the energy difference between two phases and ΔE means the activation energy which is essential for the phase transition from one to another.

absorption of laser energy. Furthermore, this high temperature can induce a high pressure inside the carbon onion by compressing the interlayer distance of carbon onions. Therefore, the carbon onion can serve as a nanoscaled temperature and pressure cell for generation of high temperature and high pressure inside the carbon onion upon laser irradiation in a liquid. Finally, the laser-induced high temperature and high pressure can induce the carbon onion to convert to the n-nanodiamond.

4. Conclusion

In summary, we demonstrated a new phase transformation from nanodiamond to n-diamond *via* an intermediate carbon onion driven by the process of laser irradiation in water, and established a thermodynamic model to elucidate the physical mechanism involved in the experimental observations. We also demonstrate that water plays a crucial role in the formation of n-diamond. These results showed that the

laser-induced high temperature in the amorphous carbon shell of the starting nanodiamonds first results in the phase transformation from the nanodiamond core to the carbon onion, and then the carbon onion is converted to the n-diamond driven by the laser-induced high temperature and high pressure from the carbon onion as a nanoscaled temperature and pressure cell upon the process of laser irradiation in a liquid. Therefore, these findings offer one suitable approach for breaking controllable pathways between n-diamond and other carbon allotropes, and open up avenues for producing n-diamonds from raw carbon materials.

Acknowledgements

The National Basic Research Program of China (2014CB931700) and the State Key Laboratory of Optoelectronic Materials and Technologies of Sun Yat-sen University supported this work.

References

- N. R. Greiner, D. S. Phillips, J. D. Johnson and F. Volk, *Nature*, 1988, **333**, 440–442.
- P. Badzic, W. S. Verwoerd, W. P. Ellis and N. R. Greiner, *Nature*, 1990, **343**, 244–245.
- F. Banhart and P. M. Ajayan, *Nature*, 1996, **382**, 433–435.
- A. De Vita, G. Galli, A. Canning and R. Car, *Nature*, 1996, **379**, 523–526.
- J.-Y. Raty and G. Galli, *Nat. Mater.*, 2003, **2**, 792–795.
- C. X. Wang, Y. H. Yang, N. S. Xu and G. W. Yang, *J. Am. Chem. Soc.*, 2004, **126**, 11303–11306.
- C. Wang, J. Chen, G. Yang and N. Xu, *Angew. Chem., Int. Ed.*, 2005, **117**, 7580–7584.
- C. X. Wang and G. W. Yang, *Mater. Sci. Eng., R*, 2005, **49**, 157–202.
- V. N. Mochalin, O. Shenderova, D. Ho and Y. Gogotsi, *Nat. Nanotechnol.*, 2012, **7**, 11–23.
- I. I. Vlasov, A. A. Shiryaev, T. Rendler, S. Steinert, S.-Y. Lee, D. Antonov, M. Voros, F. Jelezko, A. V. Fisenko, L. F. Semjonova, J. Biskupek, U. Kaiser, O. I. Lebedev, I. Sildos, P. R. Hemmer, V. I. Konov, A. Gali and J. Wrachtrup, *Nat. Nanotechnol.*, 2014, **9**, 54–58.
- H. Hirai and K.-I. Kondo, *Science*, 1991, **253**, 772–774.
- S. M. Jarkov, Y. N. Titarenko and G. N. Churilov, *Carbon*, 1998, **36**, 595–597.
- I. Konyashin, A. Zern, J. Mayer, F. Aldinger, V. Babaev, V. Khvostov and M. Guseva, *Diamond Relat. Mater.*, 2001, **10**, 99–102.
- G. Murrieta, A. Tapia and R. de Coss, *Carbon*, 2004, **42**, 771–774.
- M. L. Terranova, D. Manno, M. Rossi, A. Serra, E. Filippo, S. Orlanducci and E. Tamburri, *Cryst. Growth Des.*, 2009, **9**, 1245–1249.
- G. Baldissin and D. J. Bull, *Diamond Relat. Mater.*, 2013, **34**, 60–64.
- J. Xiao, G. Ouyang, P. Liu, C. X. Wang and G. W. Yang, *Nano Lett.*, 2014, **14**, 3645–3652.
- G. W. Yang, *Prog. Mater. Sci.*, 2007, **52**, 648–698.
- M. Fatow, I. Konyashin, V. Babaev, M. Guseva, V. Khvostov and N. Savchenko, *Vacuum*, 2002, **68**, 75–78.
- Y. Gogotsi, S. Welz, D. A. Ersoy and M. J. McNallan, *Nature*, 2001, **411**, 283–287.
- O. O. Mykhaylyk, Y. M. Solonin, D. N. Batchelder and R. Brydson, *J. Appl. Phys.*, 2005, **97**, 074302.
- S. Tomita, M. Fujii, S. Hayashi and K. Yamamoto, *Chem. Phys. Lett.*, 1999, **305**, 225–229.
- J. Cebik, J. K. McDonough, F. Peerally, R. Medrano, I. Neitzel, Y. Gogotsi and S. Osswald, *Nanotechnology*, 2013, **24**, 205703.
- E. D. Obraztsova, M. Fujii, S. Hayashi, V. L. Kuznetsov, Y. V. Butenko and A. L. Chuvalin, *Carbon*, 1998, **36**, 821–826.
- X. Li, S. Zhang, S. A. Kulinich, Y. Liu and H. Zeng, *Sci. Rep.*, 2014, **4**, 4976.
- L. Wang, S.-J. Zhu, H.-Y. Wang, S.-N. Qu, Y.-L. Zhang, J.-H. Zhang, Q.-D. Chen, H.-L. Xu, W. Han, B. Yang and H.-B. Sun, *ACS Nano*, 2014, **8**, 2541–2547.
- A. S. Barnard, S. P. Russo and I. K. Snook, *Diamond Relat. Mater.*, 2003, **12**, 1867–1872.
- P. Liu, H. Cui and G. W. Yang, *Cryst. Growth Des.*, 2008, **8**, 581–586.
- P. Liu, Y. L. Cao, C. X. Wang, X. Y. Chen and G. W. Yang, *Nano Lett.*, 2008, **8**, 2570–2575.
- S. Z. Mortazavi, P. Parvin, A. Reyhani, S. Mirershadi and R. Sadighi-Bonabi, *J. Phys. D: Appl. Phys.*, 2013, **46**, 165303.
- R. S. Lewis, T. Ming, J. F. Wacker, E. Anders and E. Steel, *Nature*, 1987, **326**, 160–162.
- V. L. Kuznetsov, A. L. Chuvalin, Y. V. Butenko, I. Y. Mal'kov and V. M. Titov, *Chem. Phys. Lett.*, 1994, **222**, 343–348.
- K.-Y. Niu, H.-M. Zheng, Z.-Q. Li, J. Yang, J. Sun and X.-W. Du, *Angew. Chem., Int. Ed.*, 2011, **50**, 4099–4102.
- M. Todt, F. G. Rammerstorfer, F. D. Fischer, P. H. Mayrhofer, D. Holec and M. A. Hartmann, *Carbon*, 2011, **49**, 1620–1627.
- F. Banhart, *Philos. Trans. R. Soc. London*, 2004, **362**, 2205–2222.